Journal of Microelectronics and Electronic Packaging (2010) **7**, 1-9
Copyright © International Microelectronics And Packaging Society
ISSN: 1551-4897

Helmholtz Resonance Based Micro Electrostatic Actuators for Compressible Gas Control: A Microjet Generator and a Gas Micro Pump

Hanseup Kim,[1,*] Khalil Najafi,[2] and Luis P. Bernal

Abstract—**This paper reports Helmholtz-resonance based micro electrostatic actuators to control compressible gaseous fluids in the micro scale. Particularly, it discusses design, fabrication, and testing results of two electrostatic actuators: a micro jet generator and an integrated peristaltic multistage micro pump. These electrostatic actuators vibrate a micro membrane in a micro chamber at a high frequency (>10 kHz), and easily induce the resonant behavior of compressible gases in the chamber. Such resonant behavior, often called the Helmholtz resonance, can repeatedly create instantaneous pressure in equilibrium between the inside and outside of the chamber and cause gas to rapidly exit the chamber, forming a collimated jet. The developed micro jet generator consists of multiple acoustic chambers in parallel; produces directional gas momentum from each chamber by utilizing the Helmholtz resonance; and collectively entrains nearby gas molecules to form a gas stream. The fabricated micro jet generator has a footprint of 1.6 × 1.6 cm^2 and contains 25 acoustic micro thrusters. It operates using a 140 V and 70 kHz sinusoidal signal and produces a thrust of 55.6 μN, a maximum air velocity of 1.2 m/s, and consumes power of 3.11 mW. The developed micro pump consists of multiple acoustic chambers in series and produces a high total pressure by accumulating pressures across the multiple chambers, while maintaining high flow rates utilizing the fluidic resonance of each pumping chamber. The fabricated 18-stage pump produces the maximum air flow rate of 4.0 sccm and maximum pressure differentials of 17.5 kPa with total power consumptions of only 57 mW. Its total package volume is 25.1 × 19.1 × 1 mm^3. It is notable that these electrostatic actuators, with their actuation membranes, acoustic chambers, fluidic channels, and micro valves, are fabricated into a single silicon chip by developing low temperature wafer bonding techniques to protect the polymer structures inside.**

Keywords—**Micro actuator, electrostatic actuation, Helmholtz resonance, microjet generator, gas micro pump, gas compressibility**

Introduction

Recent electronic devices have increasingly incorporated interfacing capability with nonelectrical environments to enhance information collection, decision-making, and even environmental stimulation abilities. Such interface allows once-computation-limited electronic devices to interact with physical environments, augment their decision-making process with direct monitoring of physical surroundings, and thus easily bridge multiple information domains, such as mechanical, thermal, optical, and fluidic to electrical. For example, the interface to human nerve systems, such as EMG (electromyogram of the muscle), ECG (electrocardiogram of the heart), ERG (electroretinogram of the retina), EOG (electrooculogram of the eye), and EEG (electroencephalogram of the brain), has allowed numerous streams of nonelectrical bio-information to be in situ monitored by computing systems [1]. The recent revolutionary Nitendo Wii game consoles have included motion sensors to react to delicate movements of users and enabled responsive interaction of computing-based software.

Among several domains, an interface with fluids has been increasingly pursued, particularly in the microscale, due to the emerging interests and demands in accessing numerous unknown phenomena in biology, physiology, and environments in the micro and nano scale [2]. Since all living and nonliving objects are always surrounded by a fluid, either gases or liquids, they can be better accessed through the media surrounding them, and thus it is critical to establish an efficient fluidic interface. A microfluidic interface enables precisely controlled sensing and manipulation of fluids and objects, especially in the micro/nano scale, providing several advantages, such as reduced sample volumes, reaction time, device sizes, cost, power, and parallel experiments for redundancy. Its applications cover various areas, including implantable drug delivery devices [3], biochemical sensing and analysis [4], flow sensor [5], metabolomics [6], crystal formation [7], fuel cell [8], and cooling for integrated circuits [9].

The microfluidic interface has been enabled by the development of microelectromechanical systems (MEMS) technology that can construct tiny micro structures using microelectronics fabrication technology and actuate them with precision. MEMS functions can be mainly realized by two groups of fluidic interface devices: micro sensors and micro actuators. Micro sensors passively collect data from fluids or subjects in them, while micro actuators actively manipulate fluid flows or target samples in the fluids. To handle fluids with a certain volume and mass, micro actuators in particular need to acquire sufficient force, pressure, and deflection from a movable micro structure, which is not a trivial problem in the micro domain where only limited amounts of such requirements are available.

Manuscript received December 2009 and accepted March 2010
[1]Electrical and Computer Engineering, University of Utah, Salt Lake City, Utah 84108
[2]Center for Wireless Integrated Microsystems, University of Michigan, Ann Arbor, Michigan 48109
*Corresponding author; email: hanseup@ece.utah.edu

Downloaded from http://meridian.allenpress.com/jmep/article-pdf/7/1/1/2247311/1551-4897-7_1_1.pdf by guest on 01 November 2022

Fluidic manipulation utilizing micro actuators can be performed either in liquids or in gases; however, the pumping of gases is much more challenging, mainly because of gas compressibility. Liquid is an incompressible fluid, and thus its pumping is predictably controlled by manipulating the speed and the stroke volume of the pumping actuation. On the other hand, gas is compressible and thus its pumping is not the exact function of pumping actuation. For example, a certain stroke volume of a micro actuator may not result in the transfer of the same volume of gases, unlike liquids; it might not be able to pump gases out at all since gases can be instantly compressed without being physically moved out.

Despite significant research effort on microactuators for fluidic control [10-26], the development of pumping technologies for compressible gases have still remained unexplored, indeed lagging behind compared with the development of liquid micro pumps [27]. This is because gas pumping is much more complicated than liquid pumping due to gases' compressibility, sealing challenges, and limited force and stroke volume available in the micro domain. Until recently, there have been only a little more than 40 conference and journal papers on gas micropumps fabricated using MEMS technology. This is a small number compared with more than 400 archival papers published on liquid micropumps.

Controllable pumping of compressible gases can be achieved by utilizing the Helmholtz resonance, as reported in our previous studies [28]. The Helmholtz resonance can repeatedly create instant pressure gradients in the chamber and provide the needed momentum to produce gas flows. Here we present our research efforts on gaseous fluidic manipulation techniques in the microscale utilizing microactuators based on MEMS technologies [29, 30]. Particularly, we report the two examples of gas microactuators that utilize the Helmholtz resonance of compressible gases to produce high-speed micro gas streams. First, we will discuss the micro jet generator for gas flow control and report the operation principle, structure, microfabrication, and testing results. Then, we will report the gas micro pump for high gas pressure generation as well as their operation principles, microfabrication, packaging, and performance.

A. Characteristic of Gas in Microfluidic Channels

The main differences between gases and liquids are the density and the atomic interactions between the molecules. The densities of two states of matter can be estimated on the order of 1 kg/m^3 and 10^3 kg/m^3 for gas and liquid, respectively. In the case of a simple molecule in unionized state, the molecules are thought to be separated by 3–4 nm (d_0), typically at equilibrium. The average distance of gas at room temperature and pressure is considered of the order of 10 d_0, and the distance in liquid on the order of d_0 [31]. The large atomic distance in the gas state is the explanation of the compressibility of gas [32]. The mechanical properties of gases and liquids greatly depend on the compressibility, and gases can be compressed to a much greater extent than liquid. Due to the large compressibility, larger volumetric changes in the gas state will be expected compared to the liquid state, under significant changes in pressure. Thus, the amount of gas pumped will not be the same as the volumetric displacement of the membrane in the pumping stage. The gas compression ratio is defined as the volumetric ratio of the stroke of an actuator over the original chamber, and is not the function of gas properties. Typically, a high compression ratio has been adopted to generate high volume displacement and thus flow rates for liquid pumping; however, such a strategy simply does not apply to gas pumping due to the compressibility [33]. This is the main difficulty for designing and operating the gas pump. In order to increase the pump performance with the determined volume displacement, a high operating frequency is usually expected to increase volume displacement per unit time [28]. However, according to the operating frequency, the pump can undergo a pressure drop or even flow reversal, and meanwhile, this phenomena was used for a bidirectional micro pump reported by R. Zengerle et al. [34]. Forward flow was prepared at a lower operating frequency (0.1–800 Hz), and a reversal of flow at higher frequency (2–6 KHz). This was explained by a phase shift between the actuator's response and the inertia of the gas mass [30, 35].

B. Helmholtz-Resonance for Gas Pumping

Helmholtz resonance is the resonance phenomenon of compressible gases in a chamber with a narrow entrance. The Helmholtz resonance phenomenon takes place as gases are driven into a chamber to increase the pressure inside by an external force. As the external force is removed, the inertia of the gas plugs at the entrance can be established because the increased pressure inside forces the gases out of the chamber through the narrow entrance. Depending on the inertia of the gas in the narrow entrance, the gases flowing out of the chamber could be overdriven and evacuate the chamber that will be left at a lower pressure inside than the outside of the chamber. Such a lowered pressure in the chamber causes gases to be reinhaled into the chamber. This process repeats until the momentum of gases is exhausted as the pressure differences decrease, like underdamped oscillators.

The Helmholtz resonance phenomenon can be established in the microdomain by constructing microchambers with an actuating wall, and can be utilized to efficiently generate compressible gas flow and pressure, despite small displacement and limited force available in the microscale [36-38]. The basic physical concept of our approach to produce controllable gas flows in the micro domain is described in Fig. 1 [29]. Our micro Helmholtz resonator actuates the movable membrane to apply external pressure to gases by expanding and compressing the chamber in a two-cycle process. In the first cycle, the membrane compresses the gas in the chamber, and ejects it through the narrow entrance, thus forming a collimated jet. In the second cycle, it expands the chamber, and draws gas back into the chamber, but in this cycle, gas does not form a collimated jet, since gas flows in from all directions around the entrance. Therefore, during each cycle, a nonzero momentum difference is produced while the same amount of gases comes in and out of the chamber. The resultant momentum difference is utilized to induce gas flows over the repeated cycles. The momentum peaks that appear at the fluidic resonance frequency at each cycle are dependent on the dimensions of the chamber and the entrance.

Downloaded from http://meridian.allenpress.com/jmep/article-pdf/7/1/1/2247311/1551-4897-7_1_1.pdf by guest on 01 November 2022

Gas pumping utilizing the Helmholtz resonance phenomenon can be understood through an analogy to an equivalent electrical LCR oscillator system that is damped and periodically driven. In the Helmholtz resonator, the closed pumping chamber induces the counter-resistance against gas plug's movement into and out of it, which corresponds to a spring (k) in a mechanical system. The gas plug at the chamber entrance provides a mass (m) of the moving object. The resultant gas resistance could represent damping (b). Each component is corresponding to electrical components of a capacitor (C), an inductor (L), and a resistor (R), respectively. Similar to the sharp peak of current that the electrical LCR system produces at the resonance frequency, the fluidic Helmholtz resonator also produces a peak of air flow at its resonance frequency, and the maximum gas flow rate and transfer occurs at resonance. Since this is a second-order system and the deflection is a function of the density, thickness, dimension, and residual stress of the membrane, when the flexural rigidity is neglected, the resonant frequency for the fundamental mode can be given as:

$$\omega = \pi \sqrt{\frac{2\tau_m}{\rho_m t_m A_m}} \tag{1}$$

where τ_m is the tension force, ρ_m is the density, t_m is the thickness, and A_m is the area of the membrane [39]. This equation provides a useful insight that we can generate a sharp peak of high-speed gas flows at a resonant frequency that can be controlled by the geometry of the resonator.

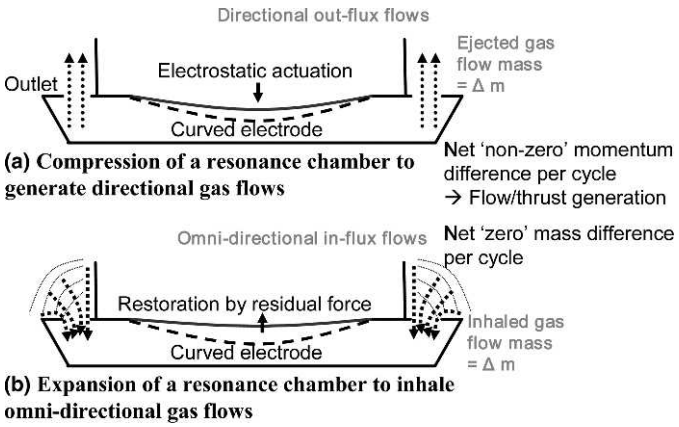


Fig. 1. Operation principle of the Helmholtz-resonance-based electrostatic micro jet generator.

C. Micro Actuators for Compressible Gas Flows

By utilizing the concept of the Helmholtz-resonance-based gas pumping, we developed micro actuators, a micro jet generator, and an integrated peristaltic micro pump, based on conventional planar microfabrication technology. These micro actuators, in common, contain the main components to realize the concept, which consist of a recessed wide cavity, a lateral entrance, and a thin membrane that covers and moves the gas in the cavity. These components are easily fabricated in 3D by utilizing conventional bulk silicon etching, DRIE technique, membrane-transfer technology, and wafer bonding. Since the micro actuators, as described in eq. (1), usually operate in a frequency range of more than tens' of KHz, they require a high-speed actuation mechanism to be capable of inducing the gas resonance at high frequency ranges. Among several potential micro actuation mechanisms, the electrostatic actuation mechanism has been chosen due to its distinct advantages of well-developed microfabrication processes, high-speed operation, material compatibility, and low power consumption, as compared in Table I.

The following sections describe the details of the two exemplary actuators for gas flow control: (1) a micro jet generator to achieve high-speed and high-flow rate gas flows (jets) and (2) a micro gas pump to achieve high gas pressure as well as high mass flow rates specifically for a micro gas chromatography application [36].

A Micro jet Generator

Micro jets have numerous potential applications, including chip cooling, gas pumping, and air-breathing micro thrusters for propulsion. For those applications, it is desirable to achieve high air velocity (and therefore high thrust), which can be produced by high-frequency and large-volume displacement of an actuation membrane at Helmholtz resonance [29, 40].

As shown in Fig. 1, the operation of the developed Helmholtz-resonance micro jet generator depends on repeated membrane movements in gas resonance. The membrane

Table I
Different operation principles for gas micro pumps

	Electrostatic	Piezoelectric	Electromagnetic	(Thermo)pneumatic	Knudsen	Motor
Control						
-Multi-ctrl	Easy	Difficult*	Difficult**	Easy	Easy	Easy
-Uniform	High	Medium	Medium	Medium	High	High
-Speed	High	High	High	Low	NA	High
Fabrication	Easy	Difficult	Difficult	Easy	Easy	Difficult
Power	Low	Low	High	High	High	High
Force	Low	High	High	High	NA	Very high
Deflection	Medium	Medium	Large	Large	NA	Very large
Volume	Small	Small	Large	Small	Small	Large
Material compatibility	High	Low	Low	Low	High	High
Temperature/humidity sensitivity	Low	High	Low	Medium	Low	Low

*Piezoelectric material should be identically fabricated in individual stages.
**Neighboring membranes should be protected from fringing magnetic field.

Downloaded from http://meridian.allenpress.com/jmep/article-pdf/7/1/1/2247311/1551-4897-7_1_1.pdf by guest on 01 November 2022

compresses and expands gases in the chamber to produce directional and unidirectional air flow at each phase of a cycle, resulting in net momentum per cycle. Each cycle repeats at a high frequency, resulting in a large net momentum generated and zero mass transfer per unit time. The operation frequency is determined by the geometry of the cavity.

A. Structures

The micro jets with 25 individual micro jet generators have been designed in a chessboard array, as shown in Fig. 2. In each individual micro jet generator, an actuation membrane is placed at the center and eight throats are distributed on four sides, two throats on each side. Under the membrane, a perforated curved electrode is located over a Helmholtz-resonance cavity. The curved electrode always maintains a small gap around the periphery between a membrane and a diaphragm and thus keeps the operation voltage low. Thus, it gradually deflects the membrane down from the edges toward the center, and thus maximizes the volume displacement of a membrane at a given low power consumption.

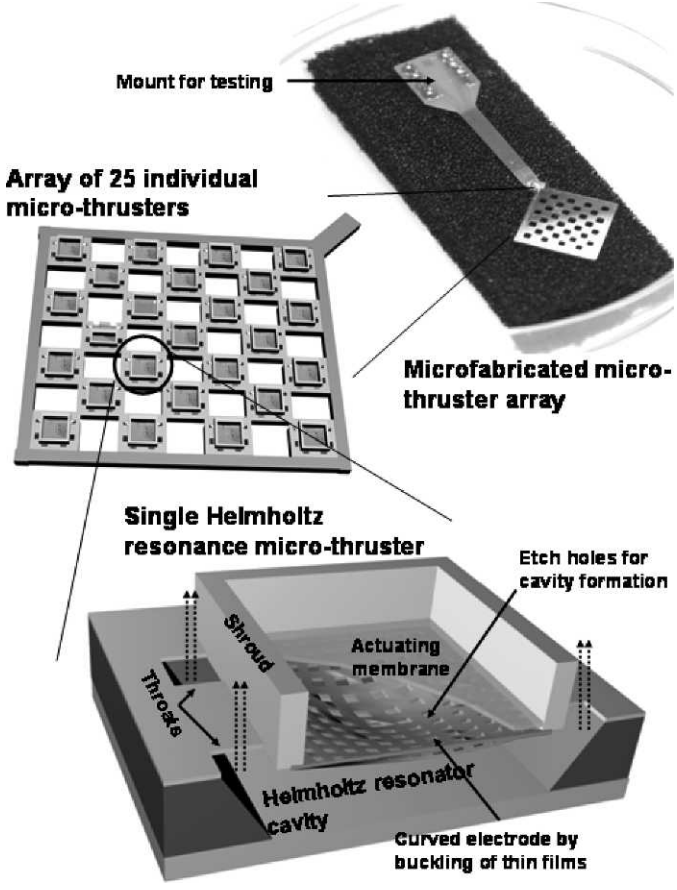


Fig. 2. (Top) A photo of the fabricated micro thruster array that is mounted on top of a PCB board. Please note that the thruster array contains 25 individual thrusters. (Middle) A 3D schematic diagram of the microfabricated micro thruster array. (Bottom) Close-up view of a single microthurster showing the components of a movable (actuating) membrane, a curved electrode, and a Helmholtz resonator cavity.

B. Fabrication

A simplified microfabrication process flow is shown in Fig. 3. First, layers of a compressively stressed thermally grown silicon oxide (0.5 μm) and LPCVD polysilicon (3.8 μm) were deposited. Then, boron doping was performed to the polysilicon layer, which provides a high resistance against the TMAH wet etching during cavity formation. On top of the doped polysilicon, a layer of tensile silicon nitride (0.1 μm) was deposited to bend the electrode downward by utilizing the stress gradient of the composite layers [29, 41]. Perforation holes were constructed in the composite layers by DRIE etching so that TMAH etchant can flow in through the holes to etch out the undoped silicon substrate part under the composite membrane. The holes can be used to reduce damping during membrane actuation as well. After the silicon substrate under the membrane was etched, the composite layers were buckled due to the intrinsic compressive stress. The buckled electrode provides a smooth curvature for low-voltage operation as well as high structural strength to prevent the unwanted bending of electrodes during electrostatic attraction [29, 41]. Then, a second wafer deposited with several films forming a movable diaphragm was bonded using BCB [39, 40]. Finally, the second wafer was DRIE-etched to release the movable diaphragm, and to form micro jet throats (holes).

C. Testing Results

First, the acoustic resonance frequency of the fabricated micro jet generators (Fig. 4) were measured by using a microphone located 2 cm above the chip. The acoustic resonant frequency is defined as the frequency where peaks appear in the acoustic spectrum, and provides an insight where the flow resonant frequency could be located. Note that the acoustic resonant frequency does not necessarily match the flow

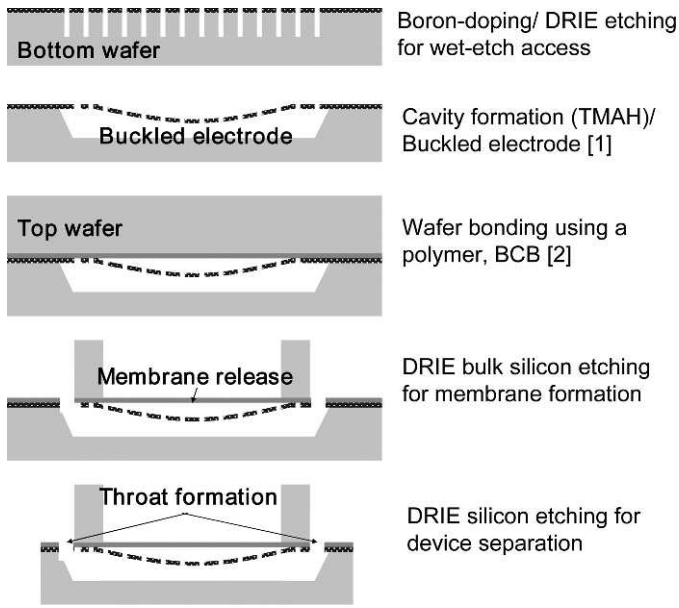


Fig. 3. Simplified wafer-level microfabrication process for a micro thruster array.

Downloaded from http://meridian.allenpress.com/jmep/article-pdf/7/1/1/2247311/1551-4897-7_1_1.pdf by guest on 01 November 2022

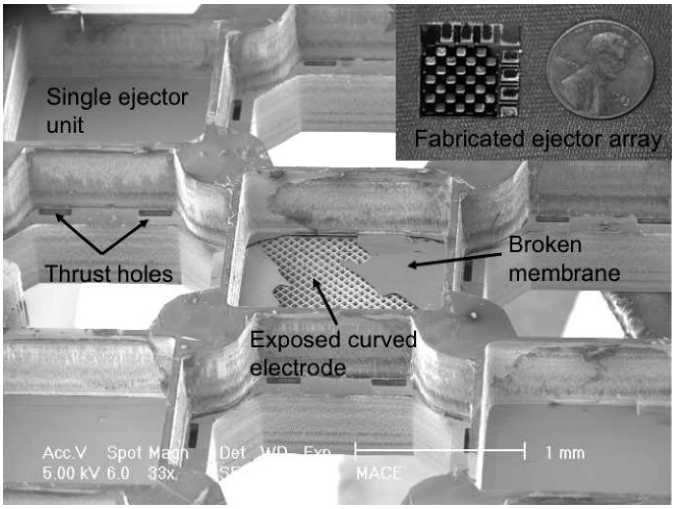


Fig. 4. SEM view of a fabricated micro thruster array, showing the actuation membrane and the underneath exposed electrode. Individual units contain two holes per side for gas flows (for a total of eight thrust holes per device).

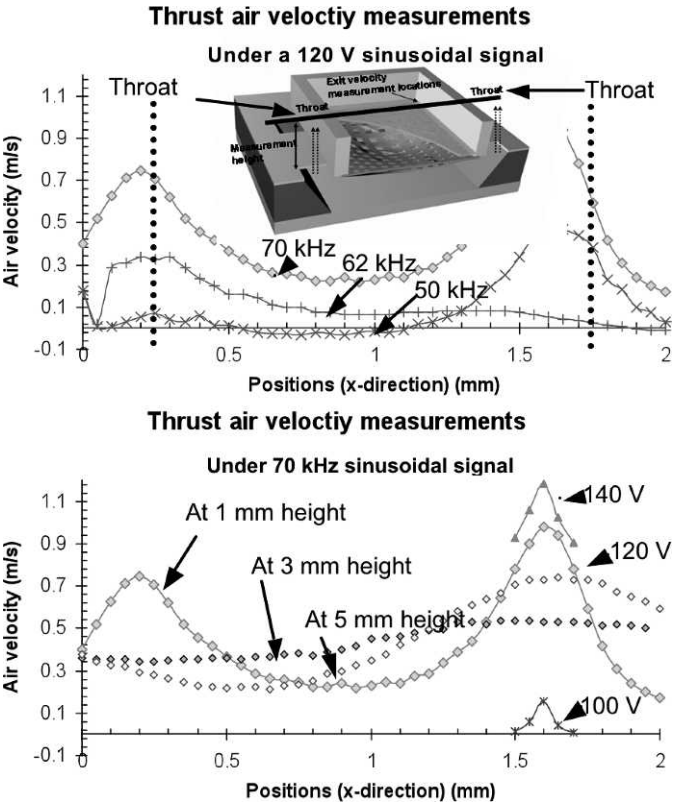


Fig. 5. (Top) Air velocity measurements across an individual micro thruster (refer to the 3D drawing) at different frequencies. Thrust values are highest over the thrust holes (throats). Thrust generation shows a maximum value at a resonance frequency of 70 kHz. (Bottom) Air velocity measurements across an individual micro thruster at different heights and voltages.

resonant frequency, possibly due to the delayed momentum transfer of gas amounts with mass. Next, to measure the air flow velocity produced by the micro thrusters, a hot-wire anemometer was placed on various locations across an individual micro jet generator, while its resistance variation was monitored. A hot-wire anemometer (TSI model 1210 T1.5) was located utilizing a three-axis micromanipulator, while the specific hot-wire test setup was calibrated through a series of wind tunnel tests to attune the relationship between resistance variation and air velocity. The anemometer was placed at various heights above the chip and at various locations across the whole chip so that it can evaluate the variation in flow velocity according to the various positions, while the variation in resistance was evaluated. The hot-wire test was also performed under various operation voltages. Ethanol vapor obtained by a commercial nebulizer was utilized for the visualization of jet flow from the micro jet generators. The thrust was also measured directly using a pendulum balance.

Test results of the air velocity created by each micro jet generator (Fig. 5) were obtained at 1 mm above the throat. The maximum air velocity was 1.2 m/s, and the average velocity over the entire device was found at around 1.0 m/s. The maximized air velocity was observed at a resonance frequency of 72 kHz, a voltage of 140 V, and a location close to the throat (1 mm high). Fig. 6 shows the jetting performance of the micro jet generator using an ethanol cloud. The ethanol cloud was obtained by a commercial nebulizer, and located under the micro jet generator array. When it was initiated, the cloud was jetted through the generator. The test of the jetting performance showed that the micro jet generators can pump an ethanol aerosol into a column up to 12 cm. Thrust performance of the micro jet generator was also assessed by attaching it to a 1.8 m long string balance. The micro jet generator array had 2.0 g of total mass including the mounts, and was operated at 70 kHz with a 140 V sinusoidal driving signal. Then, the thrust created by the micro jet generator was evaluated by measuring the moving distance of the balance. The results of the thrust performance

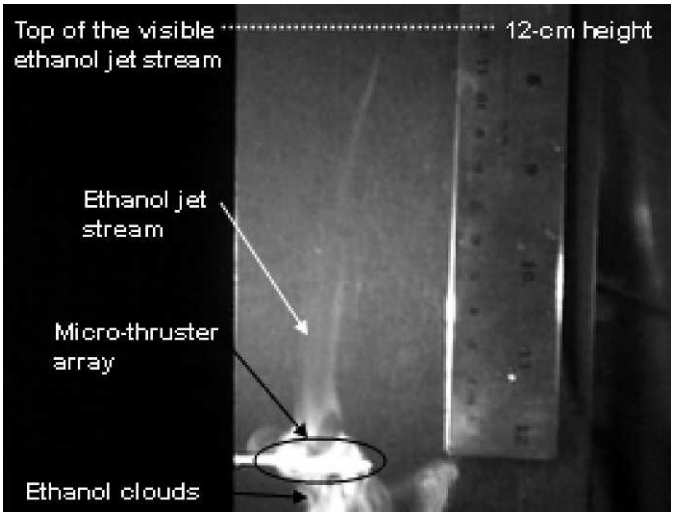


Fig. 6. Visualization of thrust generation (video clips): Ethanol jetting test results show that an ethanol column was generated vertically more than 12 cm above the chip and ethanol clouds.

showed that the micro jet array composed of 25 individual micro jet generators traveled over a distance of 4.5 mm, which corresponds to a thrust of 55.6 μN. This measured thrust value corresponds to 2.2 μN per micro jet generator.

Downloaded from http://meridian.allenpress.com/jmep/article-pdf/7/1/1/2247311/1551-4897-7_1_1.pdf by guest on 01 November 2022

D. An Integrated Peristaltic Gas Micro Pump with Active Valves

Micro-scale compressible gas pumping with high-pressure capacity is the key obstacle to various miniaturized microfluidic systems, such as laboratory-on-a-chip, because a micro device has limited force and deflection available and could not provide the needed capacity. Its development would obviate the need for bulk pumping systems, such as for large gas tanks or syringe pumps.

The Helmholtz resonator itself cannot provide sufficient pressure for most micro analytical systems, such as a micro gas chromatography (μGC) system [42]. One solution is to serially connect micro Helmholtz resonators and accumulate small pressures at each stage up to the needed high pressure across the multiple stages [30]. Note that the pressure accumulation can be achieved only by designing individual stages with a certain proper compression ratio, because individual stages experience and need to overcome exponentially distributed pressure across the multiple stages. For example, the last few stages experience much higher pressure loads than the earlier stages and must overcome the pressure for operation to prevent the overall performance degradation. We have performed theoretical studies that have shown a compression ratio of less than 7% would result in a pressure of more than 50 kPa through 18 stages [28].

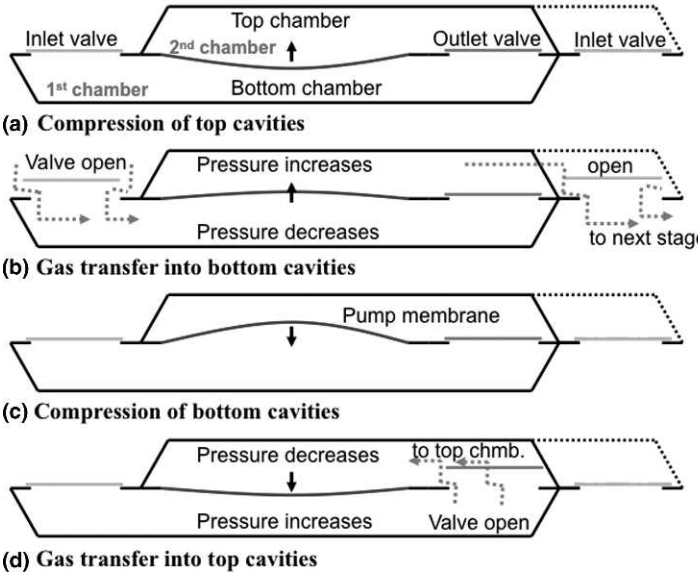
We developed a peristaltic micro pump that achieves high pressure by such pressure accumulation as well as high flow rates from the fluidic resonance utilizing the high-speed volume displacement of an electrostatically actuated membrane. Fig. 7 shows the peristaltic operation of the 18 stage micropump. In this peristaltic pump, the gas pumping is accomplished by gas drift from one chamber to the next chamber due to the pressure change. When the pumping membrane moves upward, it expands the bottom chamber, lowering the pressure in the bottom chamber with all the remaining valves closed [Fig. 7(a)]. When the pressure in the bottom chamber is dropped low enough to inhale the gas into the chamber and the inlet micro valve opens by a separate control signal, gas can be injected to the chamber [Fig. 7(b)]. After the pumping membrane reaches the top, all the valves are closed and the pumping membrane begins to move downward. It compresses the bottom chamber and increases the pressure in the chamber [Fig. 7(c)]. As the pressure in the bottom chamber reaches a level high enough for gas to transfer to the top chamber, the outlet valves are opened and the gas can be injected into the top chamber [Fig. 7(d)]. The same process repeats through the rest of the stages at the resonant frequency.

E. Structure

Nine two-stage units are serially connected to each other in the 18 stage pump, and each two-stage unit consists of two (dual) pumping chambers realized by bonding two wafers and inlet and outlet (transfer) micro valves formed between the bonded wafers. This dual pump configuration has the advantage of reducing the overall size of the pump by two pumping chambers sharing a single pumping membrane. Inlet and outlet micro valves consist of one polymer valve membrane and two silicon electrodes, all of which contain a checkerboard-type array of holes. The open or close of gas flow by the micro valves can be controlled by the match or mismatch of the holes between the valve membrane and one of the dual electrodes.

F. Fabrication

The microfabrication process for the multistage micro pump is described in Fig. 8 [43]. The main microfabrication



Mode	Inlet valves	Pump membr.	Outlet valves	Bottom chamber	Top chamber
(a)	Closed	Moving up	Closed	P↓ No flow	P↑ No flow
(b)	Open	At the top	Closed	P: min.→equilibr. In-flow	P: max.→equilibr. Out-flow
(c)	Closed	Moving down	Closed	P↑ No flow	P↓ No flow
(d)	Closed	At the bottom	Open	P: max.→equilibr. Out-flow	P: min.→equilibr. In-flow

Fig. 7. Operation principle of the reported multi-stage micropump. This figure shows only two stages for simplicity. (Left) The membrane moving sequences in four phases of top compression, gas induction, bottom compression, and gas ejection. (Right) the detailed status of each valve and pumping membrane as well as pressure and flow information in top and bottom chambers.

Downloaded from http://meridian.allenpress.com/jmep/article-pdf/7/1/1/2247311/1551-4897-7_1_1.pdf by guest on 01 November 2022

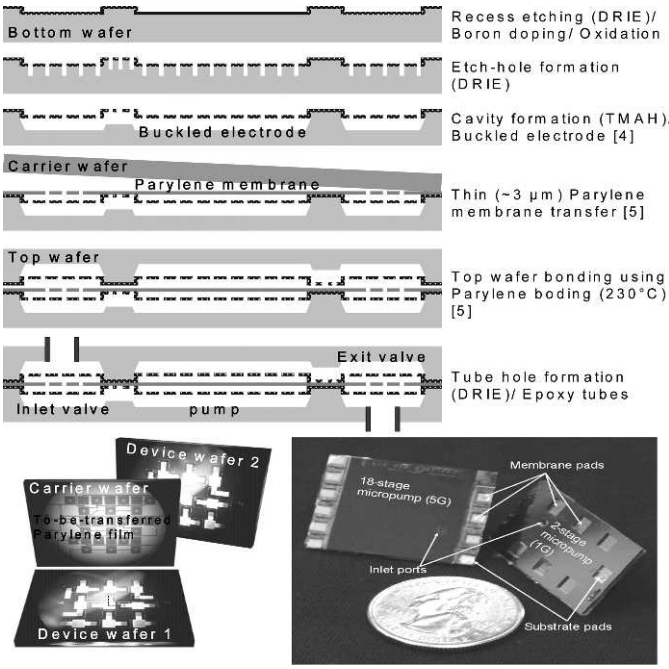


Fig. 8. (Top) Microfabrication process flow. (Bottom) The fabricated 18-stage peristaltic micro pump.

processes are wafer bonding and membrane transfer among three wafers. A carrier wafer was used for the transfer of Parylene membrane onto the device wafer, which contains pumping chambers, fluidic channels, and electrostatic electrodes. By this wafer level transfer, 1.5 μm thickness of the membrane was constructed with a 5 μm of gap between the membrane and the perforated electrode (2,000 μm) [44]. After the membrane transfer, the second device wafer was bonded to the top of the first device wafer at a relatively low temperature (∼230°C) [45]. By this bonding process, the completed pump structure was realized, sandwiching the pump and micro valve membranes between two electrodes and closing off the pump chamber.

G. Testing Results

The pumping performance of 18 stage, four stage, and two stage micro pumps operated at different voltages, frequencies, and micro valve opening duration time was evaluated by electronic mass flow meters and pressure transducers. The operation performance of the 18 stage pump at different frequencies was evaluated using a square wave voltage signal of ±100 V to determine the fluidic resonant frequency where the highest flow rate or high pressure is generated. Then, the flow versus pressure performance plot was collected with the operation of the micropumps at each resonance frequency under different load conditions. Finally, they were used to pump air to move liquid droplets and columns in order to visualize and quantify performance.

The resonance frequency peak of the 18-stage micro pump appeared at 17 kHz, and four-stage and two-stage pumps have resonance peaks at 14 kHz. The highest air flow rates of 4.0, 3.0, and 2.1 sccm were obtained with the fabricated 18-, four-, and two-stage micro pumps, respectively, as shown in Fig. 9.

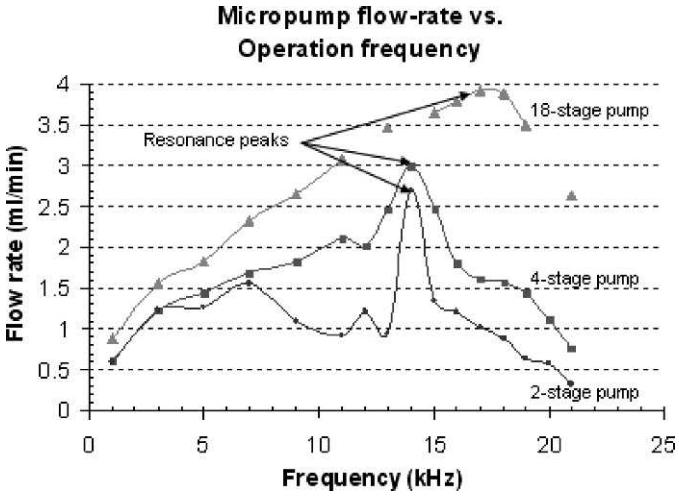


Fig. 9. Mass(gas) flow rate result measured using electronic flow meters (Omega FM1600 series) over a wide range of frequencies. An 18-stage micro pump has a resonance frequency of 17 kHz, while four-stage and two-stage pumps have resonant peaks at 14 kHz [30].

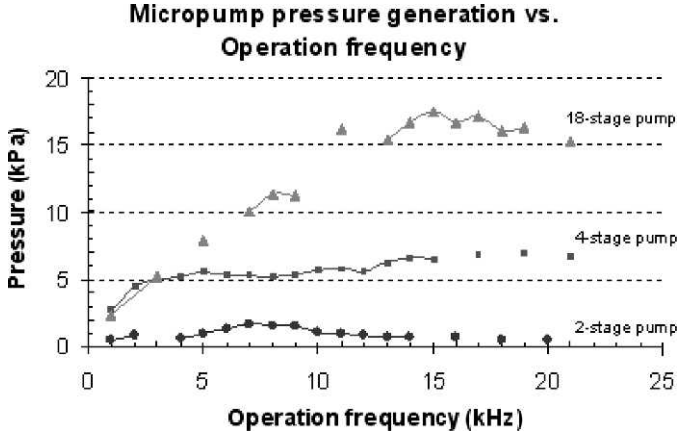


Fig. 10. Measured pressure difference over a wide range of operation frequency. The pressure was measured using electronic pressure transducers (Validyne DP-45) [30].

The energy consumed by 18-, four-, and two-stage micro pumps was measured as 57.0, 15.1, and 9.1 mW, respectively. Because the dimension of the actuating membrane for the achieved flow rates was only 2 × 2 mm^2, as a pumping efficiency is defined by the flow rate to the membrane stroke volume, this result shows the highest efficiency by any membrane-based MEMS micropump.

Fig. 10 shows the maximum pressure difference for the fabricated 18-, four-, and two-stage micropumps. The differences obtained at an operating frequency of ∼15 kHz were found to be ∼17.5, 7.0, and 2.5 kPa, respectively. It is worth noting that the operation frequencies for the maximum pressure difference were found to be different from the frequencies for the highest flow rate. Also, the maximum pressure difference increased with an increasing number of stages in the micro pump. The measured maximum pressure of 17.5 kPa is the highest pressure generated by any electrostatic MEMS micro gas pump.

Downloaded from http://meridian.allenpress.com/jmep/article-pdf/7/1/1/2247311/1551-4897-7_1_1.pdf by guest on 01 November 2022

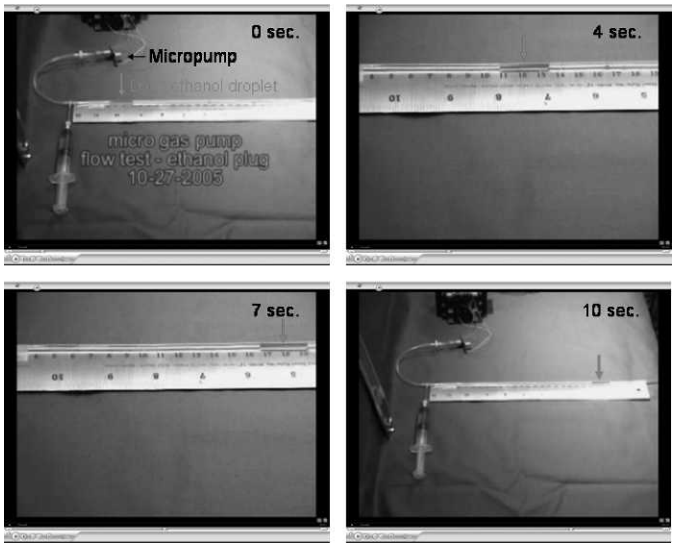


Fig. 11. Visualization: ethanol drop is pumped through a thin tube (flow rate: 1.1 sccm) using air being pumped by a gas micro pump.

The gas pumping capability of the fabricated micropumps were visualized by using liquid vapor, which was driven from one end to the other end of a tube by pumping. The liquid vapor used was ethanol, and the diameter of the tube was 1.56 mm. Fig. 11 shows a sequence of photos illustrating the movement of a liquid droplet by air being pumped behind the droplet by a four-stage pump.

Conclusion

We discussed microactuators for compressible gas flow control by taking the two examples of a microject generator and an integrated peristaltic 18-stage micro pump. These actuators utilized Helmholtz resonance to overcome the compressibility of gases and produced controllable high-speed gas flows from the microscale devices. The approaches based on the Helmholtz resonance phenomena produce a sudden peak of gas flows at the resonant frequency that is determined by the geometry and induced by a movable membrane. In order to support the resonance at a high frequency range, an electrostatic mechanism was selected.

The developed microject generator with a buckled electrode demonstrated that Helmholtz-resonance pumping can produce controllable high-speed gas flows. The fabricated micro jet generator has a footprint of 1.6×1.6 cm^2 and contains 25 acoustic microthrusters. It produces a thrust of 55.6 μN, a maximum air velocity of 1.2 m/s under 140V and 70 kHz input signal, and consumes power of 3.11 mW.

We have also developed fully integrated 18-, four-, and two-stage peristaltic electrostatic microgas pumps that (1) achieve high pressure (17.5 kPa) by accumulating pressure differences across multiple stages, (2) obtain high flow rate (4.0 sccm) by operating at a high fluidic resonance frequency (∼15 kHz) despite a small membrane size (2×2 mm^2), while consuming only small power (∼57 mW).

We conclude that a Helmholtz resonance can be induced in the microscale by utilizing high-speed microactuators and that such resonance can be utilized to produce high-capacity gas flows under precise control in the micro domain.

Acknowledgments

This research was supported by the Engineering Research Center Program of the National Science Foundation under Award Number EEC-9986866. The primary author is supported by the Utah Science Technology and Research Initiative (USTAR) program.

References

[1] J.W. Judy, "Biomedical Applications of MEMS," *Measurement and Science Technology Conference*, Anaheim, CA, p. 403, 2000.
[2] W. Wang and S.A. Soper, "*Bio-MEMS: Technologies and Applications*," Boca Raton, FL, CRC Press, 2007.
[3] D. Maillefer, H.v. Lintel, G. Rey-Mermet, and R. Hirschi, "A high-performance silicon micro pump for an implantable drug delivery system," *IEEE 12th International Conference on MEMS,* p. 541, 1999.
[4] J. Mairhofer, K. Roppert, and P. Ertl, "Microfluidic systems for pathogen sensing: A review," Sensors, Vol. 9, p. 4804, 2009.
[5] J. Wang, M. Sullivan, and S.Z. Hua, "Electrolytic bubble based flow sensor for microfluidic system," Journal of Microelectromechanical Systems, Vol. 16, p. 1087, 2007.
[6] J.R. Kraly, R.E. Holcomb, Q. Guan, and C.S. Henry, "Review: Microfluidic applications in metabolomics and metabolic profiling," Analytica Chimica Acta, Vol. 653, p. 23, 2009.
[7] J. Leng and J.B. Salmon, "Microfluidic crystallization," Lab on a Chip, Vol. 9, p. 24, 2009.
[8] E. Kjeang, N. Djilali, and D. Sinton, "Microfluidic fuel cells: A review," Journal of Power Sources, Vol. 186, p. 353, 2009.
[9] L. Jiang, J. Mikkelsen, J.M. Koo, D. Huber, S. Yao, L. Zhang, P. Zhou, J. G. Maveety, R. Prasher, J.G. Santiago, T.W. Kenny, and K.E. Goodson, "Closed-loop electroosmotic microchannel cooling system for VLSI circuit," IEEE Transactions on Components and Packaging Technologies, Vol. 25, p. 347, 2002.
[10] S.C. Terry, J.H. Jerman, and J.B. Angell, "A gas chromatographic air analyzer fabricated on a silicon wafer," IEEE Transactions on Electron Devices, Vol. 26, p. 1880, 1979.
[11] K.E. Petersen, "Fabrication of an integrated, planar silicon ink-jet structure," IEEE Transactions on Electron Devices, Vol. 26, p. 1918, 1979.
[12] G.M. Whitesides, "The origins and the future of microfluidics," Nature, Vol. 442, p. 368, 2006.
[13] A. Manz, N. Graber, and H.M. Widmer, "Miniaturized total chemical analysis systems: A novel concept for chemical sensing," Sensors and Actuators B, Vol. 1, p. 244, 1990.
[14] T. Vilkner, D. Janasek, and A. Manz, "Micro total analysis systems. Recent developments," Analytical Chemistry, Vol. 76, p. 3373, 2004.
[15] S. Shoji and M. Esashi, "Microflow devices and systems," Journal of Micromechanics and Microengineering, Vol. 4, p. 157, 1994.
[16] F. Amirouche, Y. Zhou, and T. Johnson, "Current micro pump technologies and their biomedical applications," Microsystem Technologies, Vol. 15, p. 647, 2009.
[17] N.T. Nguyen, X. Huang, and T.K. Chuan, "MEMS-micro pumps: A review," Transactions of the ASME, Vol. 124, p. 384, 2002.
[18] S.T. Chang, V.N. Paunov, D.N. Petsev, and O.D. Velev, "Remotely powered self-propelling particles and micro pumps based on miniature diodes," Nature Materials, Vol. 6, p. 235, 2007.
[19] M.M. Teymoori and E. Abbaspour-Sani, "Design and simulation of a novel electrostatic peristaltic micromachined pump for drug delivery applications," Sensors and Actuators A, Vol. 117, p. 222, 2005.
[20] J.P. Urbanski, T. Thorsen, J.A. Levitan, and M.Z. Bazant, "Fast AC electro-osmotic micro pumps with nonplanar electrodes," Applied Physics Letters, Vol. 89, 143508, 2006.
[21] C. Yamahata, C. Lotto, E. Al-Assaf, and M.A.M. Gijs, "A PMMA valveless micro pump using electromagnetic actuation," Microfluid Nanofluid, Vol. 1, p. 197, 2005.
[22] A. Richter, A. Plettner, K.A. Hofmann, and H. Sandmaier, "A micromachined electrohydrodynamic (EHD) pump," Sensors and Actuators A, Vol. 29, p. 159, 1991.

Downloaded from http://meridian.allenpress.com/jmep/article-pdf/7/1/1/2247311/1551-4897-7_1_1.pdf by guest on 01 November 2022

[23] T. Lederer, W. Hilber, and B. Jakoby, "Fast thermo-pneumatic actuation of a thin PDMS membrane using a micro Peltier-element for microfluidic applications," Elektrotechnik & Informationstechnik, Vol. 126, p. 70, 2009.
[24] T.T. Nguyen, M. Pham, and N.S. Goo, "Development of a peristaltic micro pump for bio-medical applications based on mini LIPCA," Journal of Bionics Engineering, Vol. 5, p. 135, 2008.
[25] W.L. Bernard, H. Kahn, A.H. Heuer, and M.A. Huff, "Thin-film shape-memory alloy actuated micro pump," Journal of Microelectromechanical Systems, Vol. 7, p. 245, 1998.
[26] D.A. Ateya, A.A. Shah, and S.Z. Hua, "An electrolytically actuated micro pump," The Review of Scientific Instruments, Vol. 75, p. 915, 2004.
[27] D.J. Laser and J.G. Santiago, "A review of micro pumps," Journal of Micromechanics and Microengineering, Vol. 14, p. R35, 2004.
[28] A.A. Astle, H.S. Kim, L.P. Bernal, K. Najafi, and P.D. Washabaugh, "Theoretical and experimental performance of a high frequency gas micro pump," Sensors and Actuators A, Vol. 134, p. 245, 2007.
[29] H. Kim, A. Jaregui, C. Morrison, K. Najafi, L. Bernal, and P. Washabaugh, "Low-power electrostatic micro thruster for propulsion based on Helmholtz-resonance," *Proceedings of the 20th IEEE International Conference on Micro Electro Mechanical Systems (MEMS '07)*, Kobe, Japan, pp. 127-130, 2007.
[30] H. Kim, A. Astle, K. Najafi, L. Bernal, and P. Washabaugh, "A fully integrated high-efficiency peristaltic 18-stage gas micro pump with active micro valves," *20th IEEE International Conference on Micro Electro Mechanical Systems (MEMS '07)*, Kobe, Japan, pp. 131-134, 2007.
[31] G.K. Batchelor, "*Introduction to Fluid Dynamics,* Cambridge, UK, Cambridge University Press, 2007 (Reprinted).
[32] H. Bruus, "*Theoretical Microfluidics*," Oxford, UK, Oxford University Press, 2008.
[33] T. Gerlach, "Pumping gases by a silicon micro pump with dynamic passive valves," *IEEE International Conference on Solid-State Sensors and Actuators (Transducer '97),* p. 357, 1997.
[34] R. Zengerle, J. Ulrich, S. Kluge, M. Richter, and A. Richter, "A bidirectional silicon micro pump," Sensors and Actuators A, Vol. 50, p. 81-86, 1995.
[35] H. Kim, A. A. Astle, K. Najafi, L. P. Bernal, P. D. Washabaugh, and F. Cheng, "Bi-directional electrostatic microspeaker with two large deflection flexible membranes actuated by single/dual electrodes," *2005 IEEE Sensors,* 2005.
[36] L. Rayleigh, "The theory of the Helmholtz resonator," Proceedings of the Royal Society of London. Series A, Containing Papers of a Mathematical and Physical Character, Vol. 92, pp. 265-275, 1916.
[37] C. Eckart, "Vortices and streams caused by sound waves," Physical Review, Vol. 73, pp. 68-76, 1948.
[38] P. Filippi, D. Habault, J. Lefebvre, and A. Bergassoli, "*Acoustics: Basic Physics, Theory and Methods*, New York, Academic Press, 1999.
[39] M. Muller, "Flow structure, performance and scaling of acoustic jets," Ph. D. thesis, University of Michigan, Ann Arbor, 2002.
[40] T.K.A. Chou, K. Najafi, M.O. Muller, L.P. Bernal, and P.D. Washabaugh, "High-density micromachined acoustic ejector array for micro propulsion," *International Conference on Solid-State Sensors and Actuators (Transducers '01),* pp. 890-893, 2001.
[41] H.S. Kim, K. Najafi, P.D. Washabaugh, and L.P. Bernal, "Large-deflection out-of-plane electrostatic buckled-electrode actuator," *The 12th International Conference on Solid State Sensors, Actuators, and Microsystems (Transducers '03),* Boston, MA, pp. 794-797, 2003.
[42] J.W. Choi, A. Puntambekar, C.C. Hong, C. Gao, X. Zhu, R. Trichur, J. Han, S. Chilukuru, M. Dutta, S. Murugesan, S. Kim, Y.S. Sohn, J.H. Nevin, G. Beaucage, J.B. Lee, M.G. Bissell, and C.H. Ahn, "A disposable plastic biochip cartridge with on-chip power sources for blood analysis," *The 16th IEEE MEMS Worshop (MEMS '03), Koyto, Japan,* pp. 16-19, 2003.
[43] L. Arana, S. Schaevitz, A. Franz, and M.A. Schmidt, "A microfabricated suspended-tube chemical reactor for thermally efficient fuel processing," Journal of Microelectromechanical Systems, Vol. 12, pp. 600-612, 2003.
[44] H. Kim and K. Najafi, "Characterization of a low-temperature wafer bonding using thin film Parylene," Journal of Microelectromechanical Systems, Vol. 14, pp. 1347-1355, 2005.
[45] H. Kim and K. Najafi, "Characterization of aligned wafer-level transfer of thin and flexible Parylene membranes," Journal of Microelectromechanical Systems, Vol. 16, pp. 1385-1396, 2007.

Downloaded from http://meridian.allenpress.com/jmep/article-pdf/7/1/1/2247311/1551-4897-7_1_1.pdf by guest on 01 November 2022